

11/18/94 17:20  
High-Power RF Window Design for the PEP-II B Factory\*

M. Neubauer, J. Hodgson, N. Kroll<sup>†</sup>, C. Ng, H. Schwarz, K. Skarpas  
 Stanford Linear Accelerator Center, Stanford University, Stanford, CA 94309, USA  
 R. Rimmer  
 Lawrence Berkeley Laboratory, 1 Cyclotron Road, Berkeley, CA 94720, USA

**Abstract**

We describe the design of RF windows to transmit up to 500 kW CW to the PEP-II 476 MHz cavities. RF analysis of the windows using high-frequency simulation codes are described. These provide information about the power loss distribution in the ceramic and the matching properties of the structure. Finite-element analyses of the resulting temperature distribution and thermal stresses are presented. Fabrication methods including a proposed scheme to compensate for thermal expansion stresses are discussed and hardware tests to validate this approach are described. The effects of surface coatings (intentional and otherwise) and the application of air cooling are considered.

**1. INTRODUCTION**

RF windows are used for maintaining the integrity of vacuum envelopes while being transparent to microwave energy. In PEP II they are placed in the waveguides transferring power into the RF cavities which are under vacuum. The design goals for the PEP II Cavity window is to optimize the RF and mechanical designs for reliable operation at 500 kW of CW power at 476 MHz. RF windows are typically made of ceramics which have the desired property of low microwave loss, but tend to have low thermal conductivity and weakness in tension, so often, the failure mechanism is cracking from thermally induced tensile stresses. The sources of the non-uniform thermal loadings which create these stresses are varied, for example: ohmic dielectric losses, ohmic losses in metallizing and plating, ohmic losses in wanted and unwanted surface coatings, and heat from arcing and multipactor. The PEP II window design utilizes a construction technique which is designed to constrain the window in compression, never allowing it to achieve tensile stress. This minimizes the likelihood of cracking. HFSS (HP High Frequency Structure Simulator) and MAFIA were used to model the S-parameters of various matching schemes. MAFIA was used to model RF fields, trapped modes, and calculate power dissipation. ANSYS was used for thermal and stress analysis. Cold tests were carried out on the RF design. Braze tests were initiated for testing construction details. The first high power tests of full sized windows are planned for September 1994.

**2. RF DESIGN**

The space constraints in the tunnel, the locations of the penetrations for the feed waveguides, and the positions of the RF cavities require a transition from WR2100 to 16"x9" waveguide to put the window at the de-tuned-short position, an integral number of half-wavelengths from the cavity[1].

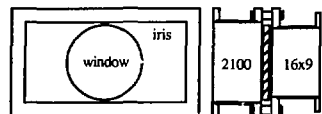
**2.1. Self Matching Window Design**

Figure 1. PEP II Self-matching window in a WR2100 to 16"x9" (406 x 23 mm) transition

A matched design was produced using a disk of 99.5% alumina in a round 254 mm diameter 38 mm long iris. The frequency and match were optimized using HFSS and MAFIA. The diameter of the window was chosen to fit within the height of the WR2100 waveguide. The thickness of the window and the length of the iris can be varied to achieve the desired match frequency. This self-matched design does not require additional tuning elements and uses the least amount of waveguide. The variation of frequency with thickness is shown in Fig. 2 for a 254 mm alumina disk of varying thicknesses in a 38 mm long iris.

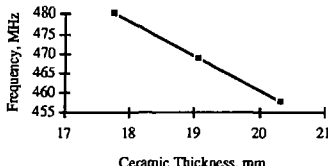


Figure 2. Match Frequency vs. Ceramic thickness for the 254 mm dia. self-matched window in 38 mm iris

Cold tests of a 254 mm disk in WR2100 were carried out using calibrated waveguide to coax transitions to compare with the calculations. The thickness and diameter of the disks in the cold tests were slightly larger than needed (and, therefore, lower in frequency) so that a final grinding operation prior to

\*Work supported by Department of Energy contracts DE-AC03-76SF00515 (SLAC), DE-AC03-76SF00098 (LBL).

<sup>†</sup>Also UCSD, DOE Grant DE-FG03-93ER40759

**DISTRIBUTION OF THIS DOCUMENT IS UNLIMITED**

metallizing would allow for fine-tuning of the required center frequency. The measured center frequency was less than one MHz from the calculated value and the VSWR less than 1.1:1 (see Fig. 3). The VSWR at the center frequency was dependent upon the alignment of the window as centered in the iris and tilted relative to that centerline (see Fig. 4).

MAFIA was used to look for trapped modes in the window as shown in Fig. 1 and the nearest mode is calculated to be 32 MHz away and outside the range of concern.

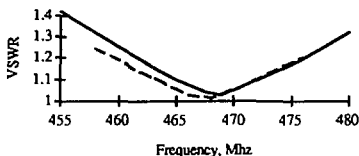


Figure 3. VSWR vs. Frequency of self-matched window (254 mm dia and 19 mm thick in 38 mm iris) in WR2100 waveguide. Comparing measured data (solid line) to MAFIA calculation (dotted line.)

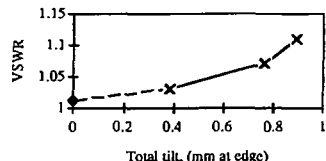


Figure 4. VSWR vs. Total tilt of window perpendicular to waveguide centerline (slant). Impact of manufacturing tolerance on the null VSWR. (♦ calculated, x measured)

## 2.2 Traveling Wave Window Design

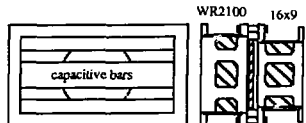


Figure 5. PEP II Traveling-wave window in WR2100 to 16x9 in waveguide transition

A further development of this design is to convert the self matching window to a traveling wave window by means of matching elements (shown in Fig. 5 as capacitive bars.) Standing waves are established between the window and these elements that exactly cancel the internal reflections at the dielectric to vacuum or air interfaces. With the design of Fig. 5, the electric field is reduced by a factor 2.7. The currents at the metallic window edge are increased by a comparable factor.

Losses in the metallization are removed efficiently by the water cooling circuit and do not contribute significantly to the stress in the ceramic.

## 3. MECHANICAL DESIGN

Under steady state conditions 174 watts are dissipated in the dielectric of the self-matched window at 500 kW incident power. This power is predominantly dissipated in the center of the ceramic and causes the ceramic to go into compression in the center while the perimeter would develop hoop tensile stress. In order to meet the design goals of a fully compressed window under any thermal condition, a compression technique was designed to place about 10 ksi (70 MPa) compressive hoop stress on the ceramic at room temperature. This is achieved by using a water cooled stainless steel compression ring that is fitted to the ceramic during brazing and contracts on cool-down.

### 3.1. Mechanical Design of the compression ring

An ANSYS model was made to determine how much steel was required in a cylinder the same length as the iris (38 mm) to produce the desired compressive stresses. The results show a cylinder with a wall thickness of at least 22 mm for a 251 mm dia window would be sufficient. The ANSYS model also predicted the ceramic might crack during cool-down from braze temperature as a result of the stresses produced at the edge and corner from differential axial contraction at the ceramic to stainless steel joint. A copper buffer layer was added and braze fillet geometry modified in the ANSYS model to reduce this strain in the yielding of the buffer layer. Braze tests were performed to investigate the buffer layer thickness and optimize a temperature cycle to minimize the axial locked in strain. The results shown in Fig. 6, indicate that a buffer layer of 5 mm is beneficial and that a hold period during cool down helps to reduce the locked in stresses by allowing for creep in the buffer layer.

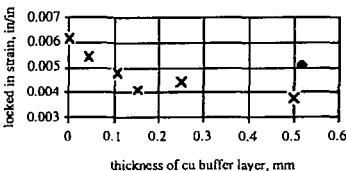


Figure 6. Braze test results for locked in strain after brazing for various thicknesses of buffer layer. Cool down from braze temperature was 1 °C per minute and, a) ♦ no hold period, b) x with a 10 hr hold period at 450 °C.

The assembly steps to accomplish making a pre-stressed window are shown in Figure 7. The stainless steel water jacket/compression ring with plated buffer layer is designed to shrink down onto the ceramic. This will be achieved with the

help of a re-usable molybdenum keeper ring. The von Mises yield strength for molybdenum is 30 ksi (210 MPa) at 1000 °C compared to 10 ksi (70 MPa) for 304 stainless steel while the coefficient of thermal expansion is  $5.6 \times 10^{-6}$  per  $C^\circ$  for molybdenum compared to  $20.3 \times 10^{-6}$  for stainless steel. In the proposed assembly the components are assembled as in Fig. 7, with the stainless steel ring between the ceramic and molybdenum keeper. On the upward temperature cycle the stainless is constrained by the stronger moly keeper until eventually it yields in compression, ending up at the same diameter as the ceramic at the braze temperature.

copper plated compression ring

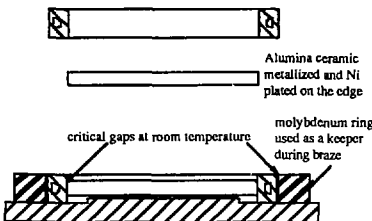


Figure 7. Window and compression ring assembly sequence

This assembly technique was simulated in ANSYS utilizing contact elements to model the gaps between the ceramic, stainless steel, and molybdenum. A one third scale model with only a stainless steel ring and molybdenum keeper was tested to see if the compressed ring diameter was reduced by the amount predicted by ANSYS. The measured room temperature diameter reduction was the same as calculated (.76 mm). The maximum elongation of the ring was twice what was calculated (.1 mm) probably due to the sticking friction between the molybdenum keeper ring and stainless steel compression ring.

The next sequence of braze tests will be on the one-third scale model including the ceramic to investigate the optimum chamfer geometry and braze fillet size. Once these tests have been done, the full size window ceramics will be ground to their final dimensions and we will attempt to braze them into compression rings.

### 3.2 Operating temperature and stress.

Using the RF heat distribution in the ceramic calculated by MAFIA, various operating and cooling conditions were modeled in ANSYS. The results of these calculations are shown in Table 1.

Once the pre-stressed window is assembled it will be coated with Titanium Nitride (TiN) to inhibit multipactor, and assembled into the WR2100 to 16x9 transition. The max. and min. window stresses expected in operation with both air and water cooling and thin film losses corresponding to a coating of 2 meg-ohm are shown in Fig. 8. These film losses are approximately worst case TiN plus undesired sputtered films.

COOLING configuration	Window center	Compression ring	$\Delta T$
	°C	°C	°C
water only	83	32	51
air only	80	58	22
air and water	66	32	34

Table 1: ANSYS calculated temperatures for the self matched window at a power dissipation of 174 watts for 500 kW RF incident and thin film losses corresponding to a coating of 2 meg-ohm

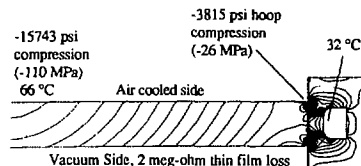


Figure 8. ANSYS contour plot of stress (2D half-symmetry) in the window at full power (500 kW).

## 4. CONCLUSIONS

According to the calculations and braze tests performed to date it should be possible to achieve our goal of a pre-stressed full size window. Use of a molybdenum keeper ring, copper buffer layer, and cool-down braze cycle reduces locked in strain in the ceramic to an acceptable level while producing the desired compression at room temperature. The margins for temperature and stress under B-factory operating conditions are substantial for the self matched window and can be further enhanced by incorporating the traveling wave window.

## 5. ACKNOWLEDGMENTS

The valuable contribution of many colleagues at SLAC, LBL and LLNL is acknowledged. The authors want to especially thank Bob Fickett, Scott Forest, and Seamus Meagher at ALTAIR Technologies for their valuable guidance in braze technology.

## 6. REFERENCES

[1] H. Schwarz et al. "RF System Design for the PEP-II B Factory." Proc EPAC 94, June 27-July 1 1994, London

## **DISCLAIMER**

This report was prepared as an account of work sponsored by an agency of the United States Government. Neither the United States Government nor any agency thereof, nor any of their employees, makes any warranty, express or implied, or assumes any legal liability or responsibility for the accuracy, completeness, or usefulness of any information, apparatus, product, or process disclosed, or represents that its use would not infringe privately owned rights. Reference herein to any specific commercial product, process, or service by trade name, trademark, manufacturer, or otherwise does not necessarily constitute or imply its endorsement, recommendation, or favoring by the United States Government or any agency thereof. The views and opinions of authors expressed herein do not necessarily state or reflect those of the United States Government or any agency thereof.